

Superconductivity and magnetism on flux-grown single crystals of NiBi₃

B. Silva,¹ R. F. Luccas,¹ N. M. Nemes,^{2,3} J. Hanco,¹ M. R. Osorio,¹ P. Kulkarni,¹ F. Mompean,^{4,5} M. García-Hernández,^{4,5}
M. A. Ramos,^{1,5} S. Vieira,^{1,5} and H. Suderow^{1,5,*}

¹Laboratorio de Bajas Temperaturas, Departamento de Física de la Materia Condensada, Instituto Nicolás Cabrera and Condensed Matter Physics Center (IFIMAC), Universidad Autónoma de Madrid, E-28049 Madrid, Spain

²Departamento de Física Aplicada III, GFMC, Universidad Complutense de Madrid, E-28040 Madrid, Spain

³Unidad Asociada Laboratorio de heteroestructuras con aplicación en espintrónica, UCM, CSIC, E-28049 Madrid, Spain

⁴Instituto de Ciencia de Materiales de Madrid, Consejo Superior de Investigaciones Científicas (ICMM-CSIC), Sor Juana Inés de la Cruz 3, 28049 Madrid, Spain

⁵Unidad Asociada de Bajas Temperaturas y Altos Campos Magnéticos, UAM, CSIC, Cantoblanco, E-28049 Madrid, Spain

(Received 13 August 2013; revised manuscript received 19 October 2013; published 13 November 2013)

We present resistivity, magnetization, and specific-heat measurements on flux-grown single crystals of NiBi₃. We find typical behavior of a type-II superconductor, with, however, a sizable magnetic signal in the superconducting phase. There is a hysteretic magnetization characteristic of a ferromagnetic compound. By following the magnetization as a function of temperature, we find a drop at temperatures corresponding to the Curie temperature of ferromagnetic amorphous Ni. Thus, we assign the magnetism in NiBi₃ crystals to amorphous Ni impurities.

DOI: [10.1103/PhysRevB.88.184508](https://doi.org/10.1103/PhysRevB.88.184508)

PACS number(s): 74.70.Ad, 74.62.Bf, 74.25.Dw

I. INTRODUCTION

The interplay between superconductivity and ferromagnetism has been one of the most fruitful areas of debate during recent years.^{1–4} The superconducting state is generally considered to be sensitive to small concentrations of magnetic impurities, which induce Cooper pair breaking.^{5–8} But, in some cases, long-range magnetic order may coexist with superconductivity.^{9,10} This leads to rather unique effects arising from the interplay between the two phenomena. Successive transitions between superconductivity and other ordered states are observed in Chevrel phase and borocarbide compounds.^{11–18} Superconducting properties have been shown to be enhanced by an external field.^{19–23} In heavy fermions and in hybrid proximity ferromagnetic-superconducting structures, magnetism can induce unconventional *p*-wave or other forms of complex superconductivity.^{24–28}

NiBi₃ is an intermetallic alloy known to be a type-II superconductor²⁹ with a critical temperature of about 4 K. Normally, Ni tends to lose its magnetic moment within this type of compound.²⁹ However, recent work shows coexistence of ferromagneticlike signals with superconductivity in polycrystalline samples.³⁰ Further work shows that ferromagnetism is absent in bulk single-crystal samples below 300 K, but that some kind of fluctuations do exist below 150 K just at the surface.³¹ In the same spirit, other authors remark the absence of ferromagnetic behavior in bulk single crystals, but show ferromagnetic and superconducting features in nanostructures. They highlight confinement effects which eventually modify the electronic band structure.³² One of the main concerns when fabricating these kinds of samples is that pure Ni inclusions can remain within the crystal, thus yielding a nonzero magnetic moment.

In this work, we have studied the superconducting properties of high-quality NiBi₃ single crystals grown by the flux-growth method. We have carried out resistivity, magnetization, and specific-heat measurements, with the aim to understand the magnetic and superconducting behavior of this system. We

indeed find a ferromagnetic signal, also in the superconducting phase, and discuss temperature dependence of magnetization, resistivity, and specific heat.

II. EXPERIMENTAL DETAILS

The sample was grown in excess of Bi flux.^{33–35} 90% high-purity Bi (Alfa Aesar 99.99%) and 10% of Ni (Alfa Aesar 99.99%) were introduced in an ampoule of quartz and sealed under inert gas atmosphere. Ampoules were heated for 4 h until 1100 °C, maintained 100 h at this temperature, and then cooled to 300 °C in 300 h, where it remained for another 100 h. Ampoules were then taken out of the furnace and rapidly centrifuged to remove the Bi flux. We obtained small needles of 0.1 mm × 0.1 mm × 1.5 mm as shown in Fig. 1. Most of these needles were joined together with residual Bi flux left over after centrifuging. We made powder x-ray diffraction on an arrangement of needles milled down to powder. We used an X'Pert PRO Theta/2Theta diffractometer with primary monochromator and fast X'Celerator detector. We measured the resistivity making four contacts on a single needle. Specific heat was determined in PPMS system of Quantum Design. To ensure proper thermalization of the whole sample, a large amount of needles (6.2 mg) were crushed down into a pellet using a force of 5.5 tons during 6 min. We made magnetization hysteresis loops *M*(*H*) at constant temperature below and above *T_c* with a SQUID magnetometer (MPMS) using single needles aligned parallel to the applied magnetic field.

III. RESULTS AND DISCUSSION

NiBi₃ has an orthorhombic CaLiSi₂-type crystal structure with space group *Pnma* and is shown in the inset of Fig. 2.³⁶ Figure 2 shows the diffraction pattern obtained at room temperature with Cu *K*_{α,1} ($\lambda = 1.54051$ Å) radiation from the powder prepared from NiBi₃ needles. The powder pattern has been fitted using the FULLPROF suite of programs implementing Rietvelds method.³⁷ The observed curve can be fitted using

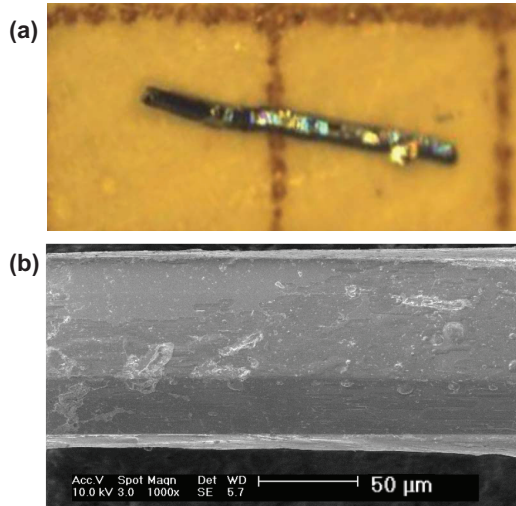


FIG. 1. (Color online) (a) NiBi_3 needle of ≈ 1.2 mm length on a millimeter paper. The needle was separated mechanically from a bunch of NiBi_3 needles joined together by Bi flux. (b) Scanning electron microscope (SEM) picture of one needle with a cross section of $0.1 \text{ mm} \times 0.1 \text{ mm}$. Some Bi flux bubbles can be identified.

two phases. A majority of $Pnma$ NiBi_3 , with refined lattice parameters $a = 8.877 \text{ \AA}$, $b = 4.097 \text{ \AA}$, and $c = 11.480 \text{ \AA}$, and a minority of rhombohedral $R\bar{3}m$ Bi, with refined lattice parameters $a = b = 4.5451 \text{ \AA}$ and $c = 11.854 \text{ \AA}$. We estimate the volume of the Bi phase to be around 0.5% from the ratio of the scale factor. In Fig. 2, the most prominent peak from the Bi phase corresponds to the reflection from 012 and is indicated with an arrow. We did not find any indication pointing to the presence of pure Ni. Note that the fit residuals around $2\theta = 30.8^\circ$ and 34.1° are large compared to the rest of the curve. This shows that some preferred crystalline orientations have not been completely eliminated when making the powder.

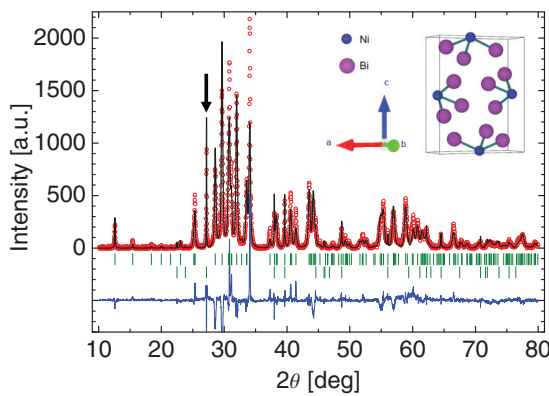


FIG. 2. (Color online) Powder diffraction pattern of NiBi_3 recorded at room temperature using $\text{Cu } K\alpha_1$ ($\lambda = 1.54051 \text{ \AA}$) radiation. Red symbols are the experimental points, connected by a red line (guide to the eye). The black line is the pattern fitted by the Rietveld method. Fit residuals are given by the blue line. The two series (upper and lower) of vertical green strikes represent, respectively, the position in 2θ scale of the reflections from the NiBi_3 ($Pnma$) and Bi ($R\bar{3}m$) phases. The arrow points at the most intense reflection from the Bi impurity.

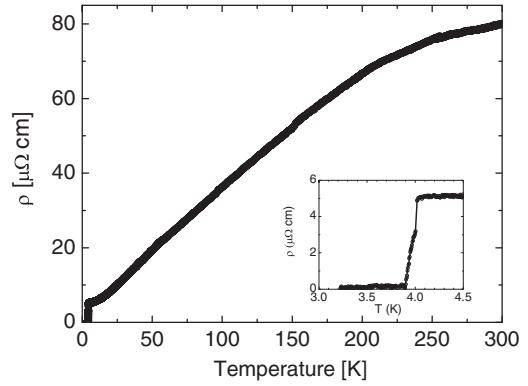


FIG. 3. In the main figure, we show the temperature dependence of the resistivity between 300 and 3.5 K. In the lower right inset, we zoom into the superconducting transition at the critical temperature.

The resistance strongly drops with decreasing temperature, and gives a residual resistance ratio between 4 and 300 K of 15.3 (Fig. 3), indicating good quality single crystal. The superconducting transition starts at 4.0 K with an abrupt drop of the resistivity and ends at 3.9 K, where it becomes zero. Previous resistance and susceptibility measurements give similar residual resistivity values in single crystals.²⁹ Critical temperature of polycrystals and in nanostructured samples is also similar.^{30–32,38}

The specific heat (Fig. 4) shows a small peak at the transition, of size expected for a weak coupling BCS superconductor, $\Delta C/T_c = 1.43\gamma$ if we take $\gamma \approx 9 \text{ mJ/K}^2 \text{ mol}$, which is compatible to the estimated zero-temperature extrapolation of C/T . The transition is sharp and located at the same temperature as the resistive transition. We find a small anomaly around 2.2 K, which depends on applied magnetic field. The contribution to the specific heat from this anomaly extends to temperatures well above the position of the kink. Actually, in a BCS superconductor, one expects the zero-field specific heat to fall below the normal-state specific heat approximately around $0.6 T_c$. Here, the zero-field specific heat remains above the 5-T specific heat over the whole temperature range. The observed anomaly at 2.2 K is of magnetic origin and of the same order than electronic and phonon contributions. A

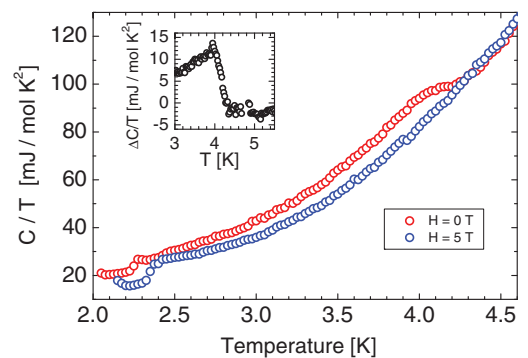


FIG. 4. (Color online) Specific heat divided by temperature C/T as a function of temperature T for NiBi_3 at zero magnetic field (red points) and at 5 T (blue points). Inset shows the jump at the superconducting transition as the difference between 5- and 0-T specific heats (ΔC).

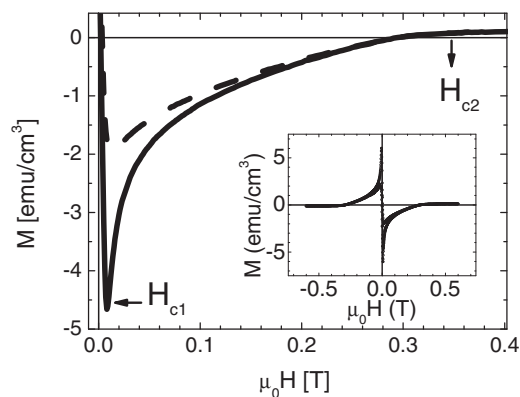


FIG. 5. Magnetization as a function of magnetic field at 1.8 K. The continuous line shows increasing field after ZFC. The dashed line shows decreasing field from 6 T. Arrows indicate the superconducting critical fields. Inset shows the full magnetization loop.

magnetic transition at this temperature involving the whole sample should give an overwhelming contribution to the specific heat.^{34,39} Therefore, this anomaly is not due to a full bulk magnetic transition but rather to residual magnetism. No traces of this transition are found in other measurements. The specific-heat measurements are the only ones made using pressed powder and not single crystals. Probably, the procedure of crushing the needles into a pellet has induced magnetism in a small part of the crushed pellet.

The main panel of Fig. 5 shows the magnetization of NiBi₃ single crystal at 1.8 K. The solid curve corresponds to the first increase of the field after zero-field cooling (ZFC) and the dashed line to a decreasing field. From the minimum in the transition between Meissner and Shubnikov states we find $\mu_0 H_{c1} = 12$ mT. The normal state is reached at $\mu_0 H_{c2} = 0.35$ T indicated by a change in the slope of $M(H)$. The magnetization curves within the superconducting state are rather closed, and we find a reversible behavior over a significant range of magnetic fields. This is expected in a high-purity single crystalline sample with low pinning. Single-crystalline samples grown by the solid-state method give small hysteresis loops,³⁰ similar to ours. Other samples grown by encapsulation of stoichiometric powder, which show grains and some inhomogeneities, also present larger hysteresis loops.³⁸ The magnetization loops with highest hysteresis were for samples grown by reductive etching of Bi₁₂Ni₄I₃.³²

From $\frac{H_{c2}(0)}{H_{c1}(0)} = \frac{2\kappa^2}{\ln(\kappa)}$ [where $H_{c1,2}(0)$ are zero-temperature extrapolations of first and second critical fields], $H_{c2}(0) = \frac{\phi_0}{2\pi\mu_0\xi^2}$ and $\kappa = \frac{\lambda}{\xi}$, we find $\kappa = 5.29 \pm 0.01$, $\xi = 300 \pm 10$ Å, and $\lambda = 1600 \pm 200$ Å. The thermodynamic critical magnetic field is $H_c(0) = 50 \pm 3$ mT [from $H_{c1}(0) = \frac{H_c(0)}{\sqrt{2}\kappa}$].

At magnetic fields above H_{c2} , the magnetization shows a peculiar behavior, characterized by a finite magnetization, typical of a ferromagnet. When we increase the temperature above T_c , we can remove the superconducting signal and find the ferromagnetic behavior. It gives hysteresis loops as shown in Fig. 6. The saturation field is small, but well defined ($M_S = 0.1417$ emu/cm³). The loops are rather closed, with a coercive field of 2.0 mT, and remanence of $M_r = 0.00872$ emu/cm³ (inset of Fig. 6). The saturation magnetization corresponds to

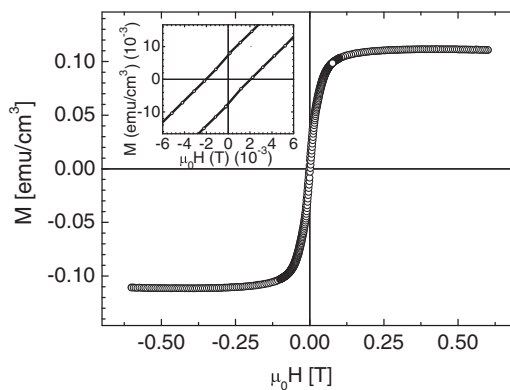


FIG. 6. Magnetization hysteresis loop at 10 K. The inset gives a zoom to highlight the behavior close to zero field. Note that the hysteresis is small, indicating soft ferromagnetism.

$\approx 1.74 \times 10^{-3} \mu_B/\text{Ni}$ as compared to the $M_S \approx 0.616 \mu_B/\text{Ni}$ of elemental ferromagnetic Ni. Thus, magnetism is residual.

As mentioned above, the magnetization curves remain closed, and we do not observe evidences for irreversibility related to magnetism. Thus, the ferromagnetic signal does not produce significant vortex pinning effect. This is compatible with the closed magnetization loop of the normal phase, i.e., with soft magnetic features as those found, for instance, in permalloy-superconductor hybrid structures.⁴⁰

We measured the magnetization of the NiBi₃ crystals up to 700 K to search for eventual high-temperature disappearance of the ferromagnetic signal (Fig. 7). We find indeed a jump and change of slope at $T = 525$ K with no further transition until 700 K. The Curie temperature of crystalline Ni is at $T_C = 631$ K. Thus, the magnetic component is not due to crystalline Ni inclusions. The lack of peaks in x-ray scattering from crystalline Ni implies that there are no crystallized Ni impurities larger than the x-ray coherence length of a few 100 Å. This, of course, does not exclude amorphous Ni. Amorphous Ni is a ferromagnet with a Curie temperature $T_C = 530$ K. This value is very close to the observed change of slope of Fig. 7.⁴¹ We thus conclude that amorphous Ni inclusions produce the observed coexistence of superconductivity and magnetism in this system.

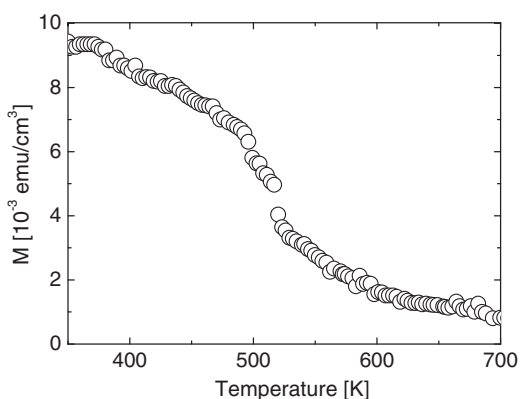


FIG. 7. Magnetization of NiBi₃ at high temperatures, in an applied magnetic field of 1 mT. Note the transition at 525 K, close to the Curie temperature of amorphous Ni.

IV. SUMMARY AND CONCLUSIONS

We have prepared NiBi₃ single crystal with the flux-growth method, which shows good type-II superconducting behavior along with ferromagnetism. We have measured resistivity, specific heat, and magnetization. Resistivity shows that we have prepared good quality single-crystalline samples, and from specific heat we obtain a full superconducting transition. In the magnetization curves we find, at the same time, superconducting and ferromagnetic signals. We have shown that the ferromagnetic signal seen in the magnetization experiments stems from amorphous Ni inclusions in the superconducting NiBi₃ matrix. Thus, the coexistence of ferromagnetism and superconductivity in this system is extrinsic. However, it is clear that this intermetallic system is prone to give, at the local scale, interesting situations where magnetism and superconductivity show some interplay. This may lead to anomalous proximity effects or vortex pinning features.^{24,42}

Comparing the observed magnetic signal per Ni atom to the expected magnetization, we obtain that about 0.3% of the volume of the sample should be ferromagnetic. It is likely that the amorphous Ni inclusions are created during growth.

Strong local variations of the superconducting density of states and anomalous proximity effect behavior should occur close to the interface between the superconductor and the ferromagnet. Vortex arrangements in the superconductor may considerably change close to such interfaces. Local measurements such as scanning squid, magnetic force, magnetic decoration, or scanning tunneling microscopies could give insight in the interplay between superconductivity and magnetism at these interfaces.

ACKNOWLEDGMENTS

We acknowledge discussions with A. I. Buzdin and F. Guinea. This work was supported by the Spanish MINECO (Grants No. FIS2011-23488, No. ACI-2009-0905, No. MAT2011-27470-C02-02, and No. CSD2009-0013) and by the Comunidad de Madrid through program Nanobiomagnet. We particularly acknowledge P. C. Canfield for teaching us the flux-growth method. We also acknowledge B. Santander for support in setting up the flux-growth bench and COST 1201 action.

*Corresponding author: hermann.suderow@uam.es

¹P. C. Canfield, P. L. Gammel, and D. J. Bishop, *Phys. Today* **51**(10), 40 (1998).

²S. A. Kivelson, G. Aeppli, and V. J. Emery, *Proc. Natl. Acad. Sci. USA* **98**, 11903 (2001).

³D. Aoki, A. Huxley, E. Ressouche, D. Braithwaite, J. Flouquet, J.-P. Brison, E. Lhotel, and C. Paulsen, *Nature (London)* **413**, 613 (2001).

⁴E. Coronado, C. Marti-Gastaldo, E. Navarro-Moratalla, A. Ribera, S. Blundell, and P. Baker, *Nat. Chem.* **2**, 1031 (2010).

⁵B. T. Matthias, *Phys. Rev.* **92**, 874 (1953).

⁶J. A. Chervenak and J. M. Valles, *Phys. Rev. B* **51**, 11977 (1995).

⁷D. Garrett, H. Beckmann, and G. Bergmann, *Phys. Rev. B* **57**, 2732 (1998).

⁸R. A. Smith and V. Ambegaokar, *Phys. Rev. B* **62**, 5913 (2000).

⁹J. Flouquet and A. Buzdin, *Phys. World* **15**, 41 (2002).

¹⁰L. N. Bulaevskii, A. I. Buzdin, M. L. Kulić, and S. V. Panjukov, *Adv. Phys.* **34**, 175 (1985).

¹¹W. A. Fertig, D. C. Johnston, L. E. DeLong, R. W. McCallum, M. B. Maple, and B. T. Matthias, *Phys. Rev. Lett.* **38**, 987 (1977).

¹²H. R. Ott, W. A. Fertig, D. C. Johnston, M. B. Maple, and B. T. Matthias, *J. Low Temp. Phys.* **33**, 159 (1978).

¹³J. W. Lynn, J. A. Gotaas, R. N. Shelton, H. E. Horng, and C. J. Glinka, *Phys. Rev. B* **31**, 5756 (1985).

¹⁴R. Prozorov, M. D. Vannette, S. A. Law, S. L. Bud'ko, and P. C. Canfield, *Phys. Rev. B* **77**, 100503 (2008).

¹⁵V. Crespo, J. G. Rodrigo, H. Suderow, S. Vieira, D. G. Hinks, and I. K. Schuller, *Phys. Rev. Lett.* **102**, 237002 (2009).

¹⁶M. Crespo, H. Suderow, S. Vieira, S. Bud'ko, and P. C. Canfield, *Phys. Rev. Lett.* **96**, 027003 (2006).

¹⁷J. Galvis, M. Crespo, I. Guillamón, H. Suderow, S. Vieira, M. G. Hernández, S. Bud'ko, and P. Canfield, *Solid State Commun.* **152**, 1076 (2012).

¹⁸M. Crespo, H. Suderow, S. Vieira, S. Bud'ko, and P. C. Canfield, *Phys. B (Amsterdam)* **378-80**, 471 (2006).

¹⁹M. B. Maple, *Phys. Today* **39**(3), 72 (1986).

²⁰S. Sangiao, J. M. De Teresa, M. R. Ibarra, I. Guillamón, H. Suderow, S. Vieira, and L. Morellón, *Phys. Rev. B* **84**, 233402 (2011).

²¹I. Guillamon, M. Crespo, H. Suderow, S. Vieira, J. P. Brison, S. L. Bud'ko, and P. C. Canfield, *Phys. C (Amsterdam)* **470**, 771 (2010).

²²H. Suderow, P. Martinez-Samper, S. Vieira, N. Luchier, J. P. Brison, and P. C. Canfield, *Phys. Rev. B* **64**, 020503 (2001).

²³R. Cordoba *et al.*, *Nat. Commun.* **4**, 1437 (2013).

²⁴A. I. Buzdin, *Rev. Mod. Phys.* **77**, 935 (2005).

²⁵F. Steglich, J. Aarts, C. D. Bredl, W. Lieke, D. Meschede, W. Franz, and H. Schäfer, *Phys. Rev. Lett.* **43**, 1892 (1979).

²⁶J.-P. Brison, L. Glémot, H. Suderow, A. Huxley, S. Kambe, and J. Flouquet, *Phys. B (Amsterdam)* **280**, 165 (2000).

²⁷F. Steglich, *Phys. B (Amsterdam)* **359-61**, 326 (2005).

²⁸F. Steglich, O. Stockert, S. Wirth, C. Geibel, H. Q. Yuan, S. Kirchner, and Q. Si, *J. Phys.: Conf. Ser.* **449**, 012028 (2013).

²⁹Y. Fujimori, S. Kan, B. Shinozaki, and T. Kawaguti, *J. Phys. Soc. Jpn.* **69**, 3017 (2000).

³⁰E. L. Martinez Piñeiro, B. L. Ruiz Herrera, R. Escudero, and L. Bucio, *Solid State Commun.* **151**, 425 (2011).

³¹X. Zhu, H. Lei, C. Petrovic, and Y. Zhang, *Phys. Rev. B* **86**, 024527 (2012).

³²T. Herrmannsdörfer, R. Skrotzki, J. Wosnitza, D. Köhler, R. Boldt, and M. Ruck, *Phys. Rev. B* **83**, 140501 (2011).

³³P. C. Canfield and Z. Fisk, *Philos. Mag. B* **65**, 1117 (1992).

³⁴P. C. Canfield, B. K. Cho, and K. W. Dennis, *Phys. B (Amsterdam)* **215**, 337 (1995).

³⁵P. C. Canfield, *Solution Growth of Intermetallic Single Crystals: a Beginner's Guide* (World Scientific, Singapore, 2009), Chap. 2, pp. 93–112.

³⁶M. Ruck and T. Z. Söhnle, *Z. Naturforsch., B: J. Chem. Sci.* **61**, 785 (2006).

- ³⁷J. Rodriguez-Carvajal, *Phys. B (Amsterdam)* **192**, 55 (1993).
- ³⁸J. Kumar, A. Kumar, A. Vajpayee, B. Gahtori, D. Sharma, P. K. Ahluwalia, S. Auluck, and V. P. S. Awana, *Supercond. Sci. Technol.* **24**, 085002 (2011).
- ³⁹L. Durivault *et al.*, *J. Phys.: Condens. Matter* **15**, 77 (2003).
- ⁴⁰Z. Yang, M. Lange, A. Volodin, R. Szymczak, and V. Moshchalkov, *Nat. Mater.* **3**, 793 (2004).
- ⁴¹K. Tamura and H. Endo, *Phys. Lett. A* **29**, 52 (1969).
- ⁴²G. Blatter, M. V. Feigel'man, V. B. Geshkenbein, A. I. Larkin, and V. M. Vinokur, *Rev. Mod. Phys.* **66**, 1125 (1994).